DALTON
FULL PAPER

# Concurrent insertion of cationic guest and solvent molecules in molecular receptors. Co-complexation of the sodium cation and acetonitrile by a calix[4]arene tetra-acetamide †

**Arvin Moser, Glenn P. A. Yap and Christian Detellier ***

*The Ottawa-Carleton Chemistry Institute, University of Ottawa, Ottawa, Ontario, Canada K1N 6N5. E-mail: dete@science.uottawa.ca*

***Received 9th February 2001, Accepted 24th October 2001***
***First published as an Advance Article on the web 4th January 2002***

The compound 5,11,17,23-tetra-*tert*-butyl-25,26,27,28-tetrakis(*N*,*N*-diethylaminocarbonyl)methoxycalix[4]arene, **1**, forms a 1 : 1 complex with the sodium cation in a binary 1 : 1 solution of chloroform-*d* and acetonitrile-$d_3$ with tetraphenylborate as the counteranion. Kinetic and mechanistic solution studies were analyzed using $^{1}$H and $^{23}$Na NMR. The formation of a 1 : 1 complex of **1** with the sodium cation is quantitative ($K_f > 10^4$ M$^{-1}$) at 238, 274, and 320 K. The exchange between complexed and solvated sodium cation is very slow on the $^{23}$Na NMR time scale even at 320 K. Analysis of 2D EXSY $^{1}$H NMR data for the interconversion of the methylene protons from the $N(CH_2CH_3)_2$ moiety of the (Na,**1**)$^+$ complex shows slow exchange at 320 K. The complexes (Na,**1**,MeCN),(Na,**1**),$(BPh_4)_2$ and (MeCN,**1**) were crystallographically characterized. X-Ray crystallographic data of (Na,**1**,MeCN),(Na,**1**),$(BPh_4)_2$ confirm the NMR data such that the sodium cation is encapsulated by the hydrophilic pseudo-cavity of **1**. The crystal structure shows two diastereomorphs of (Na,**1**)$^+$ in the lattice differing by a twist in the $OCH_2CO$ arms and only one diastereomorph contains a second guest, acetonitrile, in the hydrophobic pseudo-cavity of **1**. The crystal structure of (MeCN,**1**) shows identical preorganization of the hydrophobic pseudo-cavity to the complex (Na,**1**)$^+$.

## Introduction

Calix[4]arenes are a class of macrocyclic phenolic oligomers known to exhibit different substrate complexation selectivities *via* the modification of their substituents.[1–5a] These modifications have proven to be useful in providing compounds that exhibit selective extraction and complexation characteristics towards guests such as alkali metal cations in various solvents,[5b,c] thus providing insight into how molecular receptors adapt. Detailed kinetic and thermodynamic investigations on the complexation and decomplexation properties of the host macrocyclic molecule enable a detailed understanding on the mechanism of selectivity towards neutral, cationic, and anionic guests in solution.[1,4–7]

In this paper, the complexation of the sodium cation with the calix[4]arene tetra-acetamide, **1**, (5,11,17,23-tetra-*tert*-butyl-25,26,27,28-tetrakis(*N*,*N*-diethylaminocarbonyl)methoxycalix-[4]arene),‡ see Scheme 1, is studied using $^{1}$H and $^{23}$Na NMR spectroscopies in binary mixtures of deuterated chloroform and acetonitrile. This compound is characterized in its cone conformation by two pseudo-cavities, hydrophilic on the phenolic side, and hydrophobic on the *tert*-butyl side. The effects of the guest on the hydrophilic pseudo-cavity of **1** are discussed. In addition, the role of a neutral guest acetonitrile molecule on both (Na,**1**)$^+$ and **1** was investigated *via* X-ray crystallography.

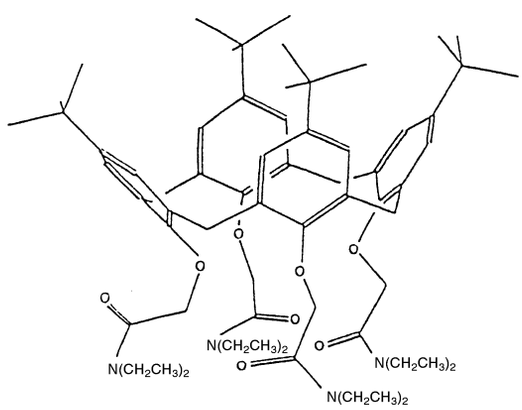


**Scheme 1**

## Experimental

### Chemicals and solutions

5,11,17,23-Tetra-*tert*-butyl-25,26,27,28-tetrakis(*N*,*N*-diethylaminocarbonyl)methoxycalix[4]arene was synthesized from NaH and *p*-*tert*-butylcalix[4]arene derivative (Aldrich 99%) as described by Arduini *et al.*[2] with an additional purification step. To ensure that all of the sodium cation was removed, the newly synthesized compound (≈0.50 g) was dissolved in 20 mL of methanol followed by 100 mL of deionized water. Subsequently, the solution was heated to evaporate the methanol leaving a white precipitate in the aqueous solution. The precipitate was collected *via* suction filtration and washed with deionized water, and dried at 110 °C for *ca*. 15 minutes. The workup was performed twice. The solid was dried for approximately 12 hours at 110 °C prior to use. Sodium tetraphenylborate (Aldrich 99.5%) was dried for about 36 hours at 110 °C prior to use.

All NMR data were obtained using a binary mixture (1 : 1 v/v). $CDCl_3$ (99.8%), $CD_3CN$ (99.8%), and $D_2O$ (99.9%) were purchased from Cambridge Isotope Laboratories. The solvents $CDCl_3$ and $CD_3CN$ were dried over 4 Å molecular sieves prior to use.

### NMR measurements

The $^{1}$H and $^{23}$Na NMR spectra were recorded on a Bruker AMX-500 spectrometer at 500.14 and 132.30 MHz, respect-

† Electronic supplementary information (ESI) available: $^{1}$H NMR of uncomplexed **1** over various temperatures. See http://www.rsc.org/suppdata/dt/b1/b101322j/

‡ IUPAC name: $1^5$,$3^5$,$5^5$,$7^5$-tetra-*tert*-$1^2$,$3^2$,$5^2$,$7^2$-tetrakis(*N*,*N*-diethylaminocarbonylmethoxy)-1,3,5,7(1,3)-tetrabenzenacyclooctaphane.

 DOI: 10.1039/b101322j

**Table 1** Crystal data and structure refinement data for (Na,**1**,MeCN),(Na,**1**),$(BPh_4)_2$,$(MeCN)_x$,$(CDCl_3)_y$ and (MeCN,**1**),MeCN

| | | |
|---|---|---|
| Empirical formula | $C_{96.5}H_{126.5}BCl_{1.5}N_6NaO_8$ | $C_{72}H_{106}N_6O_8$ |
| Formula weight | 1585.51 | 1183.63 |
| Temperature/K | 236(2) | 203(2) |
| Crystal system, space group | Tetragonal, *P*4*cc* | Monoclinic, $P2_1$ |
| *a*/Å | 18.128(2) | 11.380(2) |
| *b*/Å | 18.128(2) | 26.899(5) |
| *c*/Å | 29.457(5) | 11.468(2) |
| *β*/° | | 96.382(3) |
| Volume/Å$^3$ | 9680(2) | 3489(1) |
| *Z* | 4 | 2 |
| Density/g cm$^{-3}$ | 1.088 | 1.127 |
| Absorption coefficient/cm$^{-1}$ | 1.12 | 0.73 |
| *F* (000) | 3412 | 1288 |
| Reflections collected/unique | 75446/5085 [*R*(int) = 0.2253] | 75031/9863 [*R*(int) = 0.0420] |
| Final *R* indices [$I > 2\sigma(I)$][a] | *R*1 = 0.0759 | *R*1 = 0.1090 |
| *R* indices (all data)[a] | *R*1 = 0.1062 | *R*1 = 0.1258 |
| Absolute structure parameter | 0.6(4) | 1(2) |

[a] $R1 = \Sigma\big||F_o| - |F_c|\big|/\Sigma|F_o|$.

ively. The $^1$H NMR spectra were referenced to chloroform (7.24 ppm) and the $^{23}$Na NMR spectra were referenced to 0.02 M NaCl in 10% $D_2O$ (0 ppm at 300 K).[6] The temperature calibration was done with a thermocouple inserted in a non-spinning NMR tube containing chloroform or ethylene glycol.[6a] The error on the temperature measurements was estimated to be ± 0.5 K.

The $^1$H NMR spectra were recorded with a 90° pulse width of 6.3 μs. The acquisition time and delay between the two pulses were 4.65 and 1 s, respectively. A standard NOESY pulse sequence was used for the 2D exchange spectroscopy (2D EXSY) experiments,[6a,7,8] with a delay time of 300 ms, eight scans of 1024 points by 256 slices and a mixing time ranging from 50 to 400 ms.

The $^{23}$Na NMR spectra were recorded with a 90° pulse width of 10 μs. The acquisition times ranged from 15 to 72 ms, corresponding to sweep widths of 25 kHz. The delay time was 0.1 s (>5$T_1$ in all cases). The number of scans ranged from 1 to 5k. The longitudinal relaxation times, $T_1$, were measured by the inversion–recovery technique.[6b] A 90° pulse of 10 μs, 10 delay times (1–512 ms) and relaxation delays of at least 0.75 s were used. The data were fitted to the equation $I(t) = M_0(1 - ke^{-t/T_1})$ and $M_0$ (the macroscopic magnetic moment), $k$ (a constant), and $T_1$ determined by a nonlinear regression analysis.[6b] The $T_1$ for the solvated sodium peaks were determined at 238, 274, 300, and 320 K. They were found to be respectively 8.6(1), 16.3(1), 22.7(1), and 28.2(1) ms.

### Single-crystal X-ray diffraction

Crystals of (Na,**1**,MeCN),(Na,**1**),$(BPh_4)_2$ were obtained from a binary solution of deuterated chloroform and deuterated acetonitrile containing 20 mM $NaBPh_4$ and 5 mM **1**. The solution was allowed to slowly evaporate at ≈5 °C over a span of three months. Similarly, crystals of (MeCN,**1**) were obtained from a binary mixture of deuterated chloroform and deuterated acetonitrile containing 80 mM **1** and allowed to slowly evaporate at room temperature over a span of one month.

Crystallographic data are given in Table 1. Suitable crystals were selected, mounted on thin, glass fibers using paraffin oil and cooled to the data collection temperature. Data were collected on a Bruker AX SMART 1k CCD diffractometer using 0.3° $\omega$-scans at 0, 90, and 180° in $\varphi$. Unit-cell parameters were determined from 60 data frames collected at different sections of the Ewald sphere. Semi-empirical absorption corrections based on equivalent reflections were applied.[9a]

CCDC reference numbers 159035 and 159036.

See http://www.rsc.org/suppdata/dt/b1/b101322j/ for crystallographic data in CIF or other electronic format.

Systematic absences in the diffraction data and unit-cell parameters were consistent with *P*4*cc* and *P*4/*mcc* for (Na,**1**,MeCN),(Na,**1**),$(BPh_4)_2$, and with $P2_1$ and $P2_1/m$ for (MeCN,**1**). A thorough exploration of the centrosymmetric space group options yielded bizarre, unstable results. Solutions in the noncentrosymmetric space groups yielded computationally stable and chemically reasonable results of refinement. The structures were solved by direct methods, completed with difference Fourier syntheses and refined with full-matrix least-squares procedures based on $F^2$. Two 25% occupancy cations at four-fold rotation axes, a 50% occupancy anion at a two-fold rotation axis, a co-crystallized chloroform molecule at 25% occupancy, and three molecules of co-crystallized acetonitrile with 50, 25 and 25% occupancies were located for (Na,**1**,MeCN),(Na,**1**),$(BPh_4)_2$. Two acetonitrile molecules were found co-crystallized in (MeCN,**1**). The calix[4]arene $OCH_2CO$ arms in (MeCN,**1**) were found disordered with roughly 60/40 site occupancy distributions; three arms were disordered in the $CH_2$ moiety of $OCH_2CO$ while the remaining arm had a disordered carbonyl group. Refinement of the absolute structure parameters yielded 0.6(4) for (Na,**1**,MeCN),(Na,**1**),$(BPh_4)_2$ suggesting a 60/40 racemic twinned crystal and 1(2) for (MeCN,**1**), indicating the true hand of the data set cannot be determined. All non-hydrogen atoms were refined with anisotropic displacement parameters. All hydrogen atoms were treated as idealized contributions. All scattering factors and anomalous dispersion factors are contained in the SHELXTL 5.10 program library.[9b] Crystallographic data are given in Table 1, and selected bond lengths and angles are given in Table 2.

### Data treatment

The NMR linewidths, intensities, and chemical shifts were determined by fitting each peak with a Lorentzian lineshape. The integrals were calculated analytically using these linewidths and intensities.[6b] Lineshape analysis was performed on $^{23}$Na NMR spectra when [$Na^+$] > [**1**], using DNMR5 software.[10] The $T_2$ values of the solvated sodium, as determined from DNMR5, are within 2$\sigma$ of the $T_1$ values reported above, 8.3(2), 16.0(3), 24.5(8) and 31.0(4) ms at 238, 274, 300, and 320 K, respectively.

The integrated peaks for the 2D spectra were determined using the standard Bruker software. The volumes of the cross-peaks were normalized to the total intensities of the four peaks. The error was calculated under the assumption that the volume of the two cross-peaks should be the same. No corrections for any differences in $T_1$ were applied.[11] Exchange rates were determined by plotting the normalized volume of the cross-peak intensities for the $CH_2$ protons for the $N(CH_2CH_3)_2$ moiety of the sodium complexed species against the mixing

**Table 2** Relevant bond distances (Å) and angles (°) for (Na,**1**,MeCN)$^+$, (Na,**1**)$^+$ and (MeCN,**1**) (only the major-contributing disorder form of (MeCN,**1**) is considered). The letter A refers to an adjacent monomer and the B refers to the opposite monomer within **1**

| | | | |
|---|---|---|---|
| (Na,**1**,MeCN)$^+$ | | | |
| Na(1)–O(2) | 2.464(5) | O(2)–O(2)A | 3.081(5) |
| Na(1)–O(1) | 2.584(5) | N(1)–C(13) | 1.341(9) |
| O(1)–O(1)A | 3.213(5) | C(1)–C(53) | 4.473(8) |
| O(1)–O(2) | 2.650(5) | | |
| O(2)–Na(1)–O(2)A | 77.4(2) | O(2)–Na(1)–O(1)A | 80.3(2) |
| O(2)–Na(1)–O(2)B | 124.3(3) | O(1)–Na(1)–O(1)A | 76.9(2) |
| O(1)–Na(1)–O(2)A | 127.8(2) | O(1)–Na(1)–O(1)B | 123.1(3) |
| O(1)–Na (1)–O(2)B | 153.5(2) | C(7)–O(1)–C(12) | 111.3(5) |
| O(2)–Na(1)–O(1) | 63.3(2) | O(1)–C(12)–C(13)–O(2) | −3.0(7) |
| (Na,**1**)$^+$ | | | |
| Na(2)–O(4) | 2.477(5) | O(3)–O(4) | 2.636(5) |
| Na(2)–O(3) | 2.524(5) | O(4)–O(4)A | 3.090(5) |
| O(3)–O(3)A | 3.185(5) | N(2)–C(30) | 1.330(9) |
| O(4)–Na(2)–O(4)A | 77.2(2) | O(4)–Na(2)–O(3)A | 77.2(2) |
| O(4)–Na(2)–O(4)B | 123.8(3) | O(3)–Na(2)–O(3)A | 78.3(2) |
| O(3)–Na(2)–O(4)A | 130.3(2) | O(3)–Na(2)–O(3)B | 126.3(3) |
| O(3)–Na(2)–O(4)B | 150.4(2) | C(24)–O(3)–C(29) | 112.0(5) |
| O(4)–Na(2)–O(3) | 63.6(2) | O(3)–C(29)–C(30)–O(4) | 6.0(7) |
| (MeCN,**1**) | | | |
| C(71)–O(1), C(71)–O(5) | 3.48(2) | N(2)–C(29) | 1.45(1) |
| C(71)–O(3) | 3.43(2) | N(3)–C(46) | 1.38(1) |
| C(71)–O(7) | 3.50(2) | N(4)–C(63) | 1.51(2) |
| C(71)–O(2) | 3.84(2) | C(69)–C(17) | 4.46(1) |
| C(71)–O(4) | 3.95(2) | C(69)–C(34) | 4.51(1) |
| C(71)–O(6) | 3.60(2) | C(69)–C(51) | 4.56(1) |
| C(71)–O(8) | 4.00(2) | C(69)–C(68) | 4.54(1) |
| N(1)–C(12) | 1.50(2) | | |
| C(6)–O(1)–C(11) | 119.8(5) | O(5)–C(45)–C(46)–O(6) | 7(1) |
| O(1)–C(11)–C(12)–O(2) | 14(1) | O(7)–C(62)–C(63)–O(8) | −3(1) |
| O(3)–C(28)–C(29)–O(4) | 19.7(9) | | |

times. A slow exchange rate would fit the equation $I_{i\longrightarrow j} = k_{i\longrightarrow j}p_i\tau_{\mathbf{m}}$, and a fast exchange rate would follow the equations $I_{i\longrightarrow j} = a(1 - e^{-bm})$ and $k_{i\longrightarrow j} = ab/p_i$ where $I_{i\longrightarrow j}$ refers to the volume of the cross-peak and $p_i$ refers to the equilibrium percentage of conformer $i$.[7a,8a,b]

## Results and discussion

### Coordination studies in 1 : 1 (v/v) $CDCl_3$ : $CD_3CN$

Typical $^1$H NMR titration experiments, involving variations in the amount of $NaBPh_4$ in a 1 : 1 (v/v) $CDCl_3$ : $CD_3CN$ solution of 20 mM of compound **1**, produced new peaks resulting from the complexation of the sodium cation to **1** (Fig. 1). The singlet for the $OCH_2CO$ methylene protons (4.75 ppm) and the pair of doublets of the bridging $CH_2$ protons (4.97 and 2.92 ppm) of the uncomplexed **1** diminished as new peaks for the $OCH_2CO$ methylene protons and the bridging $CH_2$ protons evolved at a higher field (4.29 ppm, and 4.23 and 3.12 ppm, respectively). The $CH_2$ protons from the $N(CH_2CH_3)_2$ moiety exhibited two quartets at 2.91 and 3.19 ppm, respectively, upon addition of $NaBPh_4$ signifying a difference of environment between the two $CH_2$ sites. The peaks for the aromatic and the methyl protons are not shown on the NMR spectra due to obstruction by the proton peaks of the tetraphenylborate anion or because of lack of change in the position of the peaks. An excess amount of $NaBPh_4$ produced no new peaks in addition to the ones associated with the (Na,**1**)$^+$ complex (Fig. 1e–g).

Fig. 2 illustrates a linear relationship between the ratio of [$NaBPh_4$]/[**1**] and the area of the α methylene proton peaks from the $OCH_2CO$ moiety as analyzed by $^1$H NMR. The intersection point for the lines when [$NaBPh_4$] < [**1**] and [$NaBPh_4$] > [**1**] is at (1,1) for 320 K (identical results were also recorded at temperatures 238 and 274 K), therefore, indicating a quantitative complexation ($K_f > 10^4$ $M^{-1}$) at a 1 : 1 stoichiometry of **1** with the sodium guest. The complexation has been found to be quantitative at 238, 274 and 320 K. At 320 K, the linewidths of the $NCH_2$ moiety in the sodium complex broaden, showing a faster interconversion between the two methylene sites.

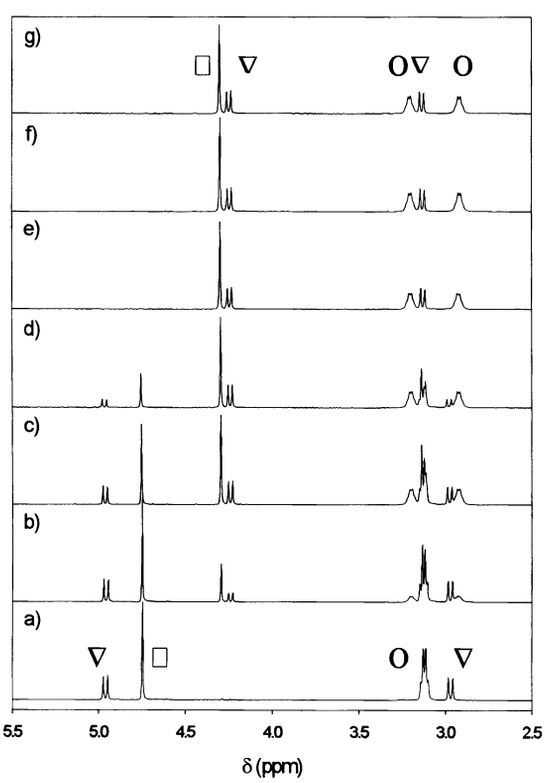


**Fig. 1** Sections of the $^1$H NMR spectra (500 MHz, 1 : 1 (v/v) $CDCl_3$ : $CD_3CN$) of 20 mM **1** in the absence (a) and in the presence (b–g) of various amounts of $NaBPh_4$ at 320 K: (b) 5, (c) 10, (d) 15, (e) 20, (f) 45, (g) 50 mM. (▽) Phenyl bridging –$CH_2$–; (□) $OCH_2CO$; (O) $NCH_2$.

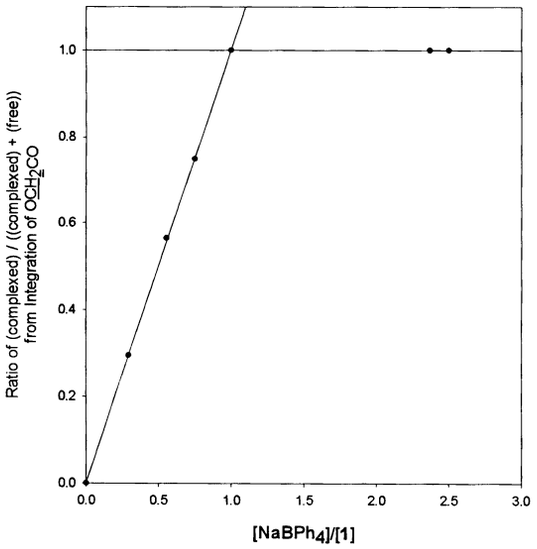


**Fig. 2** Integration ratio (complexed/(complexed + free)) for $^1$H NMR peak of $OCH_2CO$ as a function of ($[NaBPh_4]_{tot}/[\mathbf{1}]_{tot}$) at 320 K. $[\mathbf{1}]_{tot}$ = 20 mM.

Analysis of the 2D EXSY $^1$H NMR data for the interconversion of the two methylene sites from the $N(CH_2CH_3)_2$ moiety of the $(Na,\mathbf{1})^+$ complex is characterized by rate constants 0.09(2) and 1.22(2) $s^{-1}$ at 300 K and 320 K, respectively ($[NaBPh_4]$ = 20 mM and [**1**] = 15 mM). A plot of the cross-peak volumes as a function of the mixing time at 320 K describes a straight line, and no cross-peaks could be observed at 274 K.

At 320 K, the $^1$H NMR resonances (Fig. 1a) of the two methylene sites of uncomplexed **1** appear as a single quartet showing a fast exchange. The rates of exchange were determined for the temperature range of 290 to 310 K. A linear regression over five temperatures in that range afforded values for $\Delta H^{\ddagger}$ and $\Delta S^{\ddagger}$ of 105(2) kJ $mol^{-1}$ and 112(2) J $mol^{-1}$ $K^{-1}$, respectively. The free energy of activation for the two methylene sites of uncomplexed **1** was calculated to be 71(3) kJ $mol^{-1}$ at the coalescence temperature of 305 K. The result is comparable to $\Delta G^{\ddagger}$ literature values of 74.3(1.5) kJ $mol_{-1}$ for *N*,*N*-diethylacetamide at 331 K.[12]

The barrier to rotation about the C(O)–N (amide) bonds for **1** increases after complexation of sodium. For example, at 300 K, the $\Delta G^{\ddagger}$ for the interconversion is 80(2) and 72(3) kJ $mol^{-1}$, respectively for the complexed and uncomplexed **1**.

Fig. 3 shows the $^{23}$Na NMR spectra of solutions of 20 mM $NaBPh_4$ in the presence of increasing concentration of **1**. A broad line, characterized by a linewidth at half height of approximately 1.0(1) kHz, grows in at −2.11 ppm. It is attributed to the bound sodium for the 1 : 1 complex $(Na,\mathbf{1})^+$. The solvated sodium peak at −3.77 ppm disappears when [**1**] ≥ $[NaBPh_4]$ (Fig. 3f,g). The relative intensity of the solvated sodium peak decreases as [**1**] increases while maintaining the total sodium concentration, thus, verifying the 1 : 1 complexation stoichiometry observed by data from $^1$H NMR (Fig. 2). Fig. 4 shows an excellent agreement between the experimental and calculated spectra using DNMR5 at 320 K. Additional $^{23}$Na NMR spectra were recorded at temperatures 238, 255, 274 and 300 K. They showed excellent fits between the experimental and calculated spectra as analyzed by DNMR5, confirming slow exchange between bound sodium and solvated sodium occurs on the $^{23}$Na NMR time scale. The $^{23}$Na NMR data points to a strong affinity of **1** for the sodium cation. Conformational flexing of the hydrophilic pseudo-cavity appears to be small considering the lack of exchange of the sodium guest. Theoretical work *via* molecular dynamics simulation[13a] supports the notion of rigidity in the hydrophilic pseudo-cavity as a result of the encapsulation of the cation.

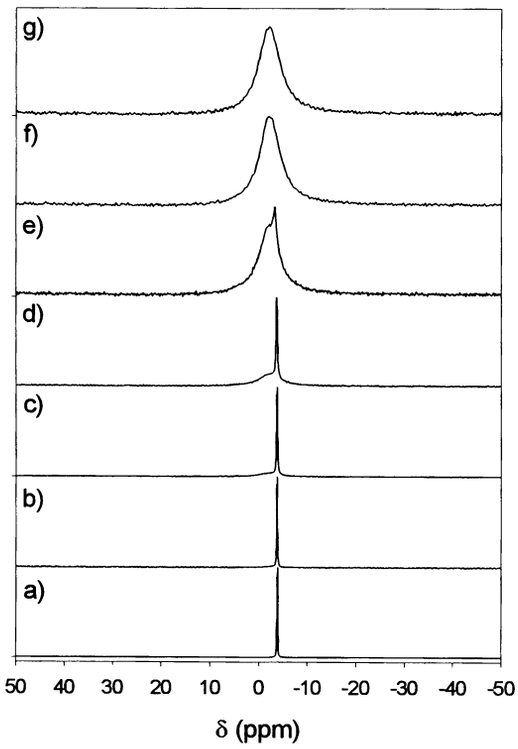


**Fig. 3** $^{23}$Na NMR spectra (132 MHz, 1 : 1 (v/v) $CDCl_3$ : $CD_3CN$) of 20 mM $NaBPh_4$ in the absence (a) and in the presence (b–f) of various amounts of **1** at 320 K: (b) 5, (c) 10, (d) 15, (e) 18, (f) 25, (g) 45 mM. The intensities for the various spectra are not on the same scale.

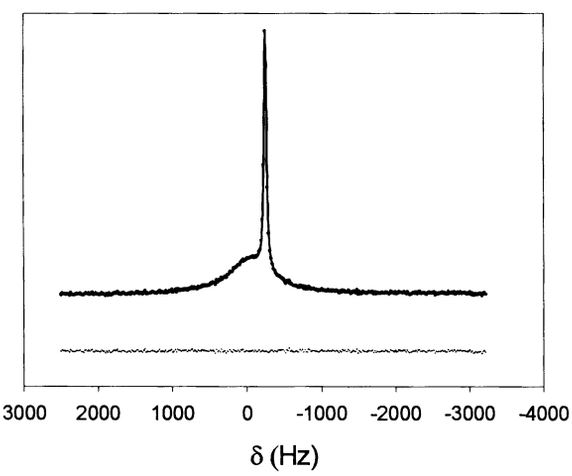


**Fig. 4** $^{23}$Na NMR spectra of 15 mM **1** and 20 mM $NaBPh_4$ at 320 K ($k$ = 0 $s^{-1}$). ● Measured spectrum, — fit with DNMR5, and — difference.

The ethyl groups form a barrier for the interactions of the complexed sodium cation with the external environment. This prevents a second sodium cation from interacting with the carbonyl groups. Previous work on the tetra{$OCH_2COCH_2CH_3$} of *p-tert*-butylcalix[4]arene and $NaBPh_4$,[6a] exhibited similar slow exchange of solvated and complexed sodium on the $^{23}$Na NMR time scale. However, the calix[4]arene appears to allow the sharing of the sodium guest with a second calix[4]arene molecule forming a 2 : 1 host–guest complex, whereas, the compound **1** forms only a 1 : 1 host–guest complex. The presence of an additional ethyl group on the nitrogen adds to the steric bulk at the entrance site of the hydrophilic pseudo-cavity. If a larger guest such as a caesium cation is used,[6b] then we expect the compound **1** to reorganize first to compensate for the large caesium cation such that the ethyl groups are pushed away from the cavity's opening. The larger the hydrophilic pseudo-cavity is, the more likely the guest will dissociate from **1**

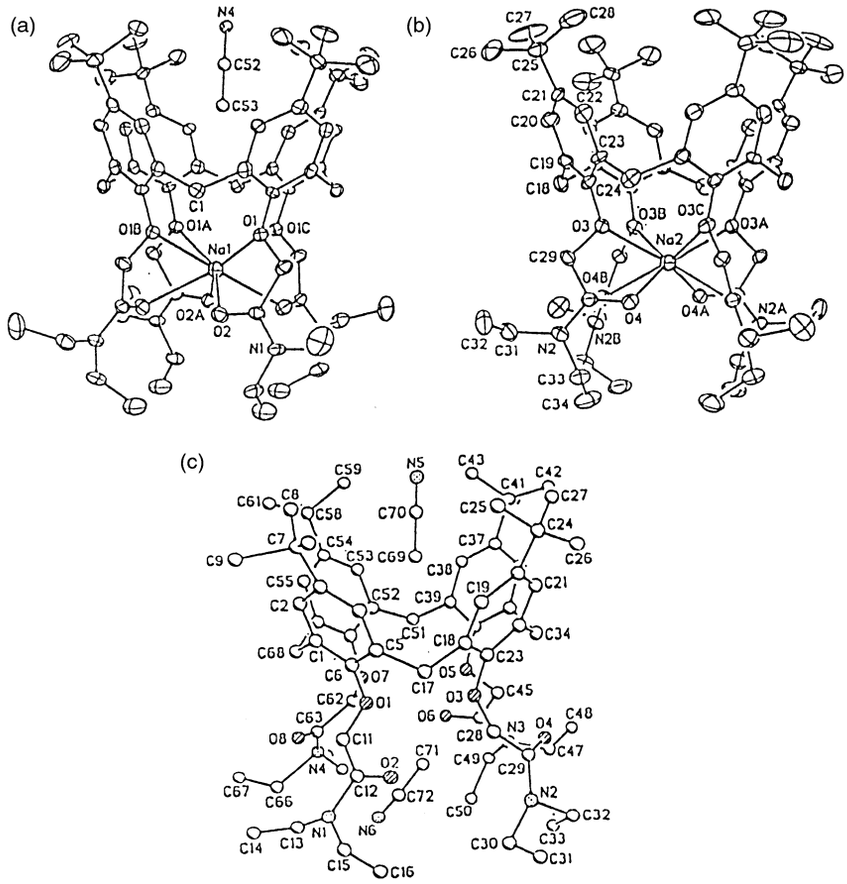


**Fig. 5** Molecular diagram of (a) 1 : 1 : 1 (Na,**1**,MeCN)$^+$, (b) 1 : 1 (Na,**1**)$^+$, and (c) 2 : 1 (MeCN,**1**) (the minor contributing disorder form for (c) is not shown). Hydrogen atoms are omitted for clarity.

as is seen for the caesium cation.[6b] The larger pseudo-cavity also exposes the carbonyl groups for a possible weak complexation with a second caesium cation. This is not observed with the solvated sodium cation.

Molecular dynamic studies by Varnek *et al.*[13] suggested an interaction of acetonitrile with the hydrophobic pseudo-cavity of **1** and its involvement in complexation of alkali metal cations. Smirnov *et al.*[14] have reported a weak complex of **1** with acetonitrile in $CCl_4$ with a stability constant of $K = 1.8\ M^{-1}$. They also suggested that the methyl group fits best in the hydrophobic pseudo-cavity of **1**. It also has been reported that the primary solvation shell is made exclusively of acetonitrile molecules.[11]

### Single-crystal X-ray analysis on (Na,1,MeCN),(Na,1),$(BPh_4)_2$

The synthetic procedure used in this work leads to compound **1** with only the cone conformation that is kinetically stable.[2] A crystallographic investigation confirms the presence of a 1 : 1 complex of sodium to **1** (Fig. 5a,b), whereby the sodium cation is encapsulated into the hydrophilic pseudo-cavity of **1**. The bond lengths, bond angles and torsion angles are presented in Table 2. The counteranion tetraphenylborate fits into the space in between the two diastereomorphs A and B, with no inclusion of the phenyl rings within the hydrophobic pseudo-cavity (Fig. 6). The crystal structure for the (Na,**1**),I previously reported by Wolf *et al.*,[15] lacked the co-complexation of a solvent molecule and possessed a high degree of disorder.

The complexes (Na,**1**,MeCN)$^+$ and (Na,**1**)$^+$ exhibit almost identical distances in the $Na^+$–$O_{amide}$, 2.464(5) and 2.477(5) Å, respectively, but vary slightly in the $Na^+$–$O_{phenolic}$ distances, 2.584(5) and 2.524(5) Å, respectively. The inclusion of an acetonitrile molecule into the hydrophobic pseudo-cavity could force the sodium from maintaining optimal interaction with the four phenolic oxygens as compared with (Na,**1**)$^+$.

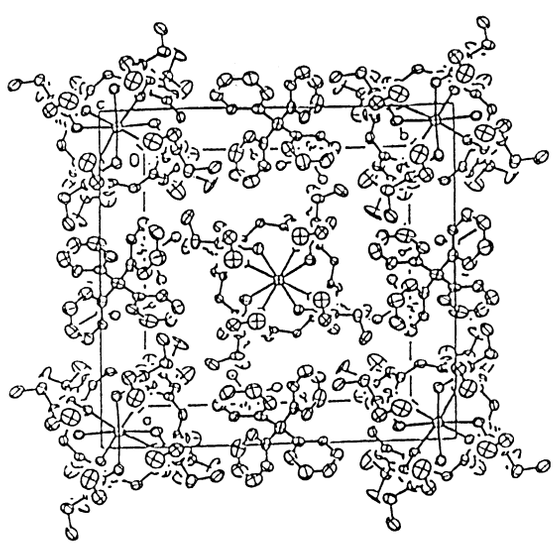

**Fig. 6** Molecular packing diagram from the perspective of the amide groups for (Na,**1**,MeCN),(Na,**1**),$(BPh_4)_2$ (the complex (Na,**1**,MeCN)$^+$ is located at the centre of the diagram with the four (Na,**1**)$^+$ complexes located at the corners). Hydrogen atoms are omitted for clarity.

As mentioned above, the lack of accessibility of a second sodium cation to the 1 : 1 complex may be accounted for by the positions of the terminal ethyl groups. This is evidenced in Fig. 6. The optimal bond lengths for $Na^+$–O create an oxygen pseudo-cavity, which in turn forces the ethyl groups to shield the pseudo-cavity's opening for access of the amide oxygen by a second sodium cation. A larger guest such as a caesium cation may expand the oxygen pseudo-cavity, and thus, remove the shielding from the terminal ethyl groups allowing access of a second caesium cation, as previously shown.[6b]

The crystallographic data exhibit two alternating diastereomorphs, A and B, that differ in the twist of the $OCH_2CO$ arms (Fig. 6). That is, diastereomorph A exhibits torsion angles in the $OCH_2CO$ arms of 6° and diastereomorph B, including acetonitrile in the hydrophobic pseudo-cavity, exhibits −3° torsion angles. The crystallographic data obtained were 60/40 racemically twinned such that the twin components are mirror images.

The X-ray data for **1** complexed with a strontium cation[16] shows a 1 : 1 complex with nearly identical oxygen-to-guest bond lengths as the sodium crystal ($Sr^{+2}$–$O_{ether}$ 2.577(5) Å avg. and $Sr^{+2}$–$O_{amide}$ 2.501(6) Å avg.). This can be attributed to the similar ionic radii of the strontium cation (1.26 Å)[17] with the sodium cation (1.18 Å).[17] However, in relation to a potassium cation (1.51 Å),[17] the bond lengths ($K^+$–$O_{ether}$ 2.708(7) Å and $K^+$–$O_{amide}$ 2.739(13) Å)[2] differ significantly due to the increase of the ionic radius. In addition, the positions of the terminal ethyl groups are directed away from the pseudo-cavity for the cations strontium and potassium, as is predicted for larger cations.

### Single-crystal X-ray analysis of (MeCN,1)

The bond lengths, bond angles and torsion angles for the (MeCN,**1**) crystal are presented in Table 2. The single-crystal structure of (MeCN,**1**) shows two acetonitriles per **1** (Fig. 5c). The high *R* value may be attributed to the poorly-packed crystal as a result of disorder in the hydrophilic pseudo-cavity of **1** and in the solvent chloroform. The bridging methylene bond angles (110.4(8)° avg.) are within experimental range to the complex $(Na,\mathbf{1})^+$ (109.2(5) and 107.7(6)° for $(Na,\mathbf{1})^+$ and $(Na,\mathbf{1},MeCN)^+$, respectively), exhibiting a preorganization by acetonitrile in the hydrophobic pseudo-cavity of **1**. Arduini *et al.*[2] reported the crystal structure of **1** with no guest in the hydrophobic pseudo-cavity such that the arrangement of the four phenyl rings lacks the four-fold rotation. The distance of the methyl carbon of the acetonitrile molecule to the bridging methylene carbons is 4.52(2) Å (avg.) whereas the distance is 4.473(8) Å for the sodium complex. The values are within experimental range of each other, thus indicating the formation of an identical hydrophobic pseudo-cavity.

The C(O)–N bond lengths of $(Na,\mathbf{1})^+$, $(Na,\mathbf{1},MeCN)^+$ and (MeCN,**1**) are 1.330(9), 1.341(9) and 1.46(2) (avg.) Å, respectively. The amide bonds are significantly longer than those seen with the sodium complex. The complexation of a cationic guest generates an increased double bond character on the C–N bonds. The shorter bond length supports the dynamic $^1H$ NMR data obtained from the exchange rate of the methylene moieties.

The positioning of the acetonitrile in the hydrophilic pseudo-cavity is a result of a polarity effect. The slightly positive methyl group in acetonitrile is oriented inside the pseudo-cavity as predicted by molecular dynamic studies.[13a] The methyl carbon in acetonitrile is closer to the phenolic oxygens than the amide oxygens, 3.45(2) (avg.) and 3.85(2) (avg.) Å, respectively. The nitrogen is directed towards one of the monomers forcing both ethyl groups of the $N(CH_2CH_3)_2$ moiety to point away from the pseudo-cavity (Fig. 7). The torsion angles for the $OCH_2CO$ arms differ significantly. The acetonitrile is directed towards one of the arms, O(7)–C(62)–C(63)–O(8), forcing it into a counterclockwise torsion angle of −3(1)°.

In conclusion, the host **1** encapsulates a sodium cation in a ratio of 1 : 1 with a very slow exchange of the guest on the $^{23}Na$ NMR time scale. Crystallographic data show the presence of an acetonitrile molecule inside the hydrophobic pseudo-cavity of **1** such that the organization of the *tert*-butyl carbons in the sodium complex is identical to that of (MeCN,**1**). In respect to the NMR data, the sodium cation is competing with the acetonitrile for the hydrophilic pseudo-cavity. The high formation constant for the sodium complex demonstrates no significant competition from the acetonitrile molecules. The conformational flexibility of the host's pseudo-cavity is highly adaptable and varies in size to accommodate different guests. Moreover, upon formation of the complex, slight variations of the structure of the host to accommodate the guest and/or solvent molecules can result in dramatic changes in the nature of the supramolecular structures being formed.

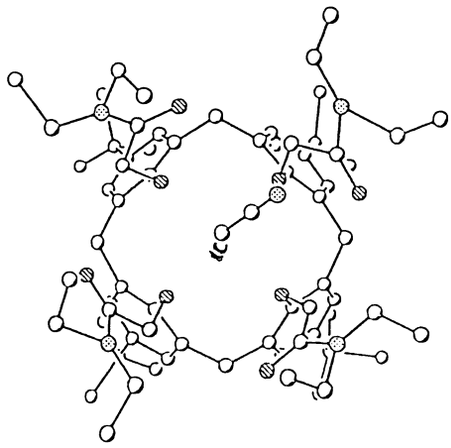

**Fig. 7** Molecular diagram from the perspective of the amide groups of 2 : 1 (MeCN,**1**) (the minor contributing disorder form is not shown). Hydrogen atoms are omitted for clarity.


## Acknowledgements

Dr Glenn C. M. Facey and Raj Capoor are thanked for their help in recording NMR spectra. Dr Urs C. Meier and Dr Yael Israëli are thanked for their help in using DNMR5.


## References


1 (*a*) C. D. Gutsche, *Acc. Chem. Res.*, 1983, **16**, 161; (*b*) C. D. Gutsche, in *Calixarenes*, ed. J. F. Stoddart, Royal Society of Chemistry, Cambridge, 1989, pp. 149–185; (*c*) V. Bohmer, *Angew. Chem., Int. Ed. Engl.*, 1995, **34**, 713; (*d*) M. Takeshita and S. Shinkai, *Bull. Chem. Soc. Jpn.*, 1995, **68**, 1088.

2 A. Arduini, E. Ghidini, A. Pochini, R. Ungaro, G. D. Andretti, G. Calestani and F. Ugozzoli, *J. Inclusion Phenom.*, 1988, **6**, 119.

3 (*a*) F. Arnaud-Neu, M. J. Schwing-Weill, K. Ziat, S. Cremin, S. J. Harris and M. A. McKervey, *New J. Chem.*, 1991, **15**, 33; (*b*) F. Arnaud-Neu, E. M. Collins, M. Deasy, G. Ferguson, S. J. Harris, B. Kaitner, A. Lough, M. A. McKervey, E. Marques, B. L. Ruhl, M. J. Schwing-Weill and E. M. Seward, *J. Am. Chem. Soc.*, 1989, **111**, 8681; (*c*) F. Arnaud-Neu, G. Barrett, S. Cremin, M. Deasy, G. Ferguson, S. J. Harris, A. Lough, L. Guerra, M. A. McKervey, M. J. Schwing-Weill and P. Schwinte, *J. Chem. Soc., Perkin Trans. 2*, 1992, 1119.

4 C. Detellier, in *Comprehensive Supramolecular Chemistry*, ed. G. Gokel, Elsevier Science, Oxford, 1996, vol. 1, pp. 357–375.

5 (*a*) F. Arnaud-Neu, G. Barrett, D. Corry, S. Cremin, G. Ferguson, J. F. Gallagher, S. J. Harris, M. A. McKervey and M. J. Schwing-Weill, *J. Chem. Soc., Perkin Trans. 2*, 1997, 575; (*b*) F. Arnaud-Neu, G. Barrett, S. Fanni, D. Marrs, W. McGregor, M. A. McKervey, M. J. Schwing-Weill, V. Vetrogon and S. Wechsler, *J. Chem. Soc., Perkin Trans. 2*, 1995, 453; (*c*) F. Arnaud-Neu, S. Fanni, L. Guerra, W. McGregor, K. Ziat, M. J. Schwing-Weill, G. Barrett, M. A. McKervey, D. Marrs and E. M. Seward, *J. Chem. Soc., Perkin Trans. 2*, 1995, 113.

6 (*a*) Y. Israëli and C. Detellier, *J. Phys. Chem. B*, 1997, **101**, 1897; (*b*) U. C. Meier and C. Detellier, *J. Phys. Chem. A.*, 1999, **103**, 3825; (*c*) U. C. Meier and C. Detellier, *J. Phys. Chem. A*, 1999, **103**, 9204.

7 (*a*) J. Blixt and C. Detellier, *J. Am. Chem. Soc.*, 1994, **116**, 11957; (*b*) J. Blixt and C. Detellier, *J. Am. Chem. Soc.*, 1995, **117**, 8536.

8 (*a*) C. L. Perrin and T. J. Dwyer, *Chem. Rev.*, 1990, **90**, 935; (*b*) J. Jeener, B. H. Meier, P. Bachmann and R. R. Ernst, *J. Chem. Phys.*, 1979, **71**, 4546; (*c*) R. R. Ernst, G. Bodenhausen and A. Wokaun, in *Principles of Nuclear Magnetic Resonance in One and Two Dimensions*, Clarendon Press, Oxford, 1987.

9 (*a*) R. Blessing, *Acta Crystallogr., Sect. A*, 1995, **51**, 33; (*b*) G. M. Sheldrick, SHELXTL, version 5.10, Bruker AXS, Madison, WI, 1997.

10 D. S. Stephenson and G. Binsch, *Quantum Chem. Prog. Exch.*, 1978, **11**, 365.
11 U. C. Meier and C. Detellier, *J. Phys. Chem. A*, 1998, **102**, 1888.
12 (*a*) T. M. Siddall, W. E. Stewart and F. C. Knight, *J. Phys. Chem.*, 1970, **74**, 3580; (*b*) A. Gryff-Keller, J. Terpinski and E. Zajaczkowska-Terpinska, *J. Chem. Res. (S)*, 1984, 330.
13 (*a*) P. Guilbaud, A. Varnek and G. Wipff, *J. Am. Chem. Soc.*, 1993, **115**, 8298; (*b*) A. Varnek and G. Wipff, *J. Phys. Chem.*, 1993, **97**, 10840.
14 S. Smirnov, V. Sodorov, E. Pinkhassik, J. Havliček and I. Stibor, *Supramol. Chem.*, 1997, **8**, 187.
15 N. J. Wolf, E. M. Georgiev, A. T. Yordanov, B. R. Whittlesey, H. F. Koch and D. M. Roundhill, *Polyhedron*, 1999, **18**, 885.
16 N. Muzet, G. Wipff, A. Casnati, L. Domiano, R. Ungaro and F. Ugozzoli, *J. Chem. Soc., Perkin Trans. 2*, 1996, 1065.
17 *CRC Handbook of Chemistry and Physics*, ed. D. R. Lide, CRC Press, Boca Raton, FL, 1998, ch. 12, pp. 14–16.